

# A Study on the Sulfur-Resistant Catalysts for Water Gas Shift Reaction

## IV. Modification of CoMo/ $\gamma$ -Al<sub>2</sub>O<sub>3</sub> Catalyst with K

Jin-Nam Park,<sup>†</sup> Jae-Hyun Kim, and Ho-In Lee\*

School of Chemical Engineering, Seoul National University, Seoul 151-744, Korea

Received October 12, 2000

The effect of K addition to the catalyst of CoMo/ $\gamma$ -Al<sub>2</sub>O<sub>3</sub> was studied. The catalyst with 10 at% of K to Mo atoms in 3C10M, the catalyst added 3 wt% CoO to 10 wt% MoO<sub>3</sub>/ $\gamma$ -Al<sub>2</sub>O<sub>3</sub>, showed the highest activity for water gas shift reaction. The addition of K retarded the reducibility of cobalt-molybdenum catalysts. It gave, however, good dispersion and large BET surface area to the catalysts which were attributed to the disappearance of polymolybdate cluster such as Mo<sub>7</sub>O<sub>24</sub><sup>6-</sup> and the formation of small MoO<sub>4</sub><sup>2-</sup> cluster. It was confirmed by the analyses of pore size distribution, activation energy, Raman spectroscopy, and electron diffraction. The activation energies and the frequency factors of the catalysts 3C10M and 5K3C10M (the catalyst added 5 at% K for Mo to the catalyst 3C10M) were 43.1 and 47.8 kJ/mole, and 4,297 and 13,505 sec<sup>-1</sup>, respectively. These values were also well correlated with our suggestion. These phenomena were attributed to the direct interaction between K and CoMo oxides irrelevant to the support.

### Introduction

The amount of carbon resources, mainly petroleum, has been continuously diminished. Many researchers have studied the development of alternative carbon sources. Those activities were concentrated on the utilization of coal or heavy crude oil such as bitumen as a novel carbon source. One of the main usage of coal is coal gasification to produce syngas.<sup>1</sup> The quality of syngas produced from coal gasification is not good for methane synthesis because the ratio of CO/H<sub>2</sub> is over 1. Therefore, water gas shift reaction process is needed for the conversion of excess carbon monoxide to hydrogen<sup>2,3</sup>; however, commercial catalysts are not applicable for the water gas shift reaction of syngas derived from coal because they are easily deactivated by impurities such as sulfur and chlorine compounds.<sup>4</sup>

To overcome the deactivation by those impurities, some researchers have studied sulfided forms of cobalt-molybdenum and nickel-molybdenum supported on  $\gamma$ -Al<sub>2</sub>O<sub>3</sub> which showed good catalytic activity in the presence of sulfur.<sup>3,5-9</sup> It has been known that the addition of alkali metal to cobalt-molybdenum catalyst enhanced the catalytic activity for water gas shift reaction and there are several postulates of the reason. Ramaswamy *et al.* reported that the addition of Na enhanced the reducibility of a catalyst.<sup>10</sup> According to his report, cobalt was not reduced at 700 K, however, it could be reduced to metal in a Na added catalyst. Lycourghiotis *et al.* reported that the addition of Li to CoMo/ $\gamma$ -Al<sub>2</sub>O<sub>3</sub> lowered the activity for hydrodesulfurization (HDS).<sup>11</sup> Kordulis *et al.* studied the effect of alkali metal on the electronic state of Mo on  $\gamma$ -Al<sub>2</sub>O<sub>3</sub> to find that the addition of any alkali metal inhibited the reduction of Mo<sup>6+</sup> to Mo<sup>5+</sup>, which depended on

the size and concentration of alkali metal.<sup>12</sup> He also found that the addition of alkali metal with the exception of Li changed octahedrally coordinated Mo<sup>6+</sup> to tetrahedrally coordinated Mo<sup>6+</sup>. Kantschewa *et al.* reported that the addition of K to NiMo/ $\gamma$ -Al<sub>2</sub>O<sub>3</sub> lowered the activity for HDS due to the decreased amount of NiMoS active sites by shattering surface heteropolymolybdate and enhanced the activity for water gas shift reaction due to stabilization of formate (a reaction intermediate) by Mo<sup>5+</sup> stabilized with K.<sup>13</sup> Kettmann *et al.* reported that K<sub>2</sub>Mo<sub>2</sub>O<sub>7</sub> was formed by the addition of K to CoMo/ $\gamma$ -Al<sub>2</sub>O<sub>3</sub> and there was no relationship between K and Co,<sup>14</sup> while Xie *et al.* reported a different result that the addition of K enhanced the reducibility of Mo catalysts.<sup>15</sup>

In the present study, we investigated why the addition of K gave the enhanced activity of water gas shift reaction to CoMo/ $\gamma$ -alumina catalyst. For the characterization of various catalysts, BET surface area, pore size distribution, TPR (temperature-programmed reduction), TEM, EDP (electron diffraction pattern), and Raman spectroscopy were analysed. We reported here that the role of K in CoMo/ $\gamma$ -alumina catalyst was different from that of Co in Mo/ $\gamma$ -alumina catalyst.

### Experimental Section

**Preparation of Catalysts.** A series of xK3C10M catalysts were prepared by co-impregnation of  $\gamma$ -Al<sub>2</sub>O<sub>3</sub> (Catalysis Society of Japan, JRC-ALO-2) with an aqueous solution of (NH<sub>4</sub>)<sub>6</sub>Mo<sub>7</sub>O<sub>24</sub> · 4H<sub>2</sub>O (Oriental, EP), Co(NO<sub>3</sub>)<sub>2</sub> · 6H<sub>2</sub>O (Shinyo, EP), and the desired amount of KNO<sub>3</sub> (Kanto, EP). The value x is the atomic percent of K to Mo atoms of the catalyst 3C10M which means the catalyst added with 3 wt% CoO to 10 wt% MoO<sub>3</sub>/ $\gamma$ -Al<sub>2</sub>O<sub>3</sub>. Water was removed by a rotary vacuum evaporator at 50 °C. And the samples were dried in air at 105 °C for 2 hours, and finally calcined at 500 °C for 5 hours.

**Catalytic Activity Test.** Sulfidation was performed before

<sup>†</sup>Present address: Department of Chemical Engineering, University of Waterloo, Waterloo, Ontario, Canada N2L 3G1

\*To whom all correspondence should be addressed. e-mail: hilee@snu.ac.kr

water gas shift reaction experiment because the calcined catalysts are in oxide form. The calcined catalyst was loaded on 100-mesh quartz frit (10 mm of diameter) located inside a quartz tube. The amount of the catalyst was 300 mg. Reactor temperature was raised to 450 °C under N<sub>2</sub> flow and 50% H<sub>2</sub>/H<sub>2</sub>S (20 mL/min) flow was introduced for sulfidation for 1 hour. After sulfidation the reactor temperature was dropped to 400 °C under N<sub>2</sub> flow to remove residual H<sub>2</sub>S for 30 min. Water was introduced by a syringe pump (Keun-A Co., KASP005/150MT). The inlet and outlet of the reactor was kept over 120 °C to prevent the condensation of water. Reaction temperature was 400 °C and flow rates of water, CO, and N<sub>2</sub> were 7, 7, and 14 mL/min, respectively. Products were analyzed by on-line GC (Packard Co.) equipped with TCD. Charcoal packed column (60-80 mesh, 1/8 in. × 2 m) was used for the analysis of the products. Catalytic activity was calculated with a following equation.

$$\text{CO conversion (\%)} = \frac{\text{CO}_{\text{in}} - \text{CO}_{\text{out}}}{\text{CO}_{\text{in}}} \times 100$$

**BET Surface Area and Pore Size Distribution Analysis.** Nitrogen (99.99%) and helium (99.99%) were used as an adsorbate and an inert gas, respectively in a commercial BET apparatus (Quantasorb M). ASAP 2000 (Micromeritics) was utilized for the pore size distribution analysis of the catalysts.

**TPR Analysis.** TPR apparatus was used to investigate the surface structure and the oxidation state of samples. The schematic diagram of TPR apparatus was shown in previous paper.<sup>16</sup> For this experiment, 40 mg of a sample was placed on a sintered quartz frit (10 mm of diameter) located inside a quartz tube. For the reduction of the sample, a H<sub>2</sub> (1.5 mL/min)/N<sub>2</sub> (28.5 mL/min) flow gas was used and heating rate was 10 °C/min.

**TEM and EDP Analysis.** Transmission electron micrographs (TEM) were taken on a JEM 100C electron microscope operating at 100 kV. The samples for TEM were prepared by dispersing a large number of the catalysts through a slurry in isopropanol onto a holey carbon film on Ni microgrids. Electron diffraction pattern (EDP) was used to confirm the crystallinity of the metal oxide on the catalysts.

**Raman Analysis.** Laser Raman spectra of the samples were obtained at room temperature using a spectrophotometer involving an Ar ion laser (540 nm, Spectra Physics, Model 2016) and a double monochromator (Spex Ramalog, Model 1403). The samples were pressed into the form of pellets at a pressure of about 50 MPa for 2 minutes because supported samples showed very low signal intensity. Smooth data of Raman analysis were acquired through a peak-fitting program.

## Results and Discussion

**Catalytic Activity:** A series of 3C10M samples with different K loading were prepared to study the effect of an alkali metal on the catalytic activity for water gas shift reac-

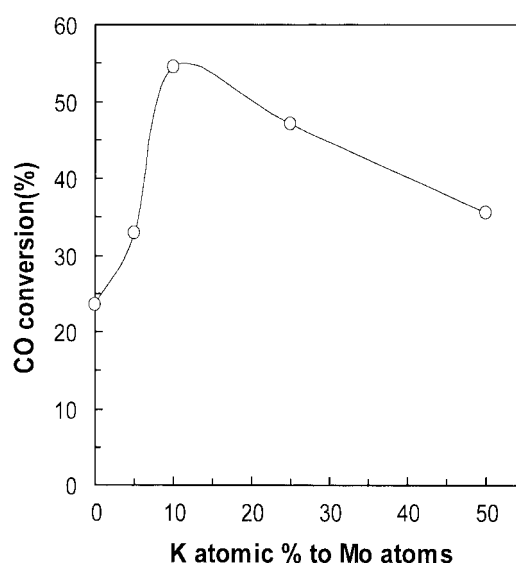


**Figure 1.** CO conversion of xK3C10M with different loading amounts of K.

tion. There have been several reports about the increase of the activity for water gas shift reaction by the addition of alkali metals, however, there is no exact explanation yet as described previously.<sup>10-15</sup> Figure 1 shows the activity for water gas shift reaction of the catalysts. It showed a volcano shape with the loading amount of K. The optimum amount of K added was 10 at% K to Mo atoms in 3C10M system. Another experiment was also carried out using 50K10M catalyst to check the effect of Co. Figure 2 shows that there was no remarkable increase of catalytic activity. 50K3C Catalyst (the amount of K is the same as that in 50K10M) also showed no enhancement of catalytic activity by the addition of K. From these results, we concluded that K did not give any enhanced catalytic activity of Mo or Co only loaded catalyst, which suggested that the coexistence of Co and Mo was important for the positive effect of the addition of K. For the comparison of catalytic activity, we also tested Fe-Cr

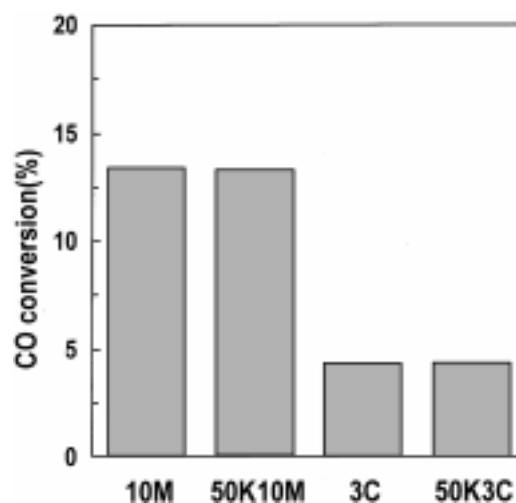


**Figure 2.** CO conversion of (a) 10M, (b) 50K10M, (c) 3C, and (d) 50K3C.

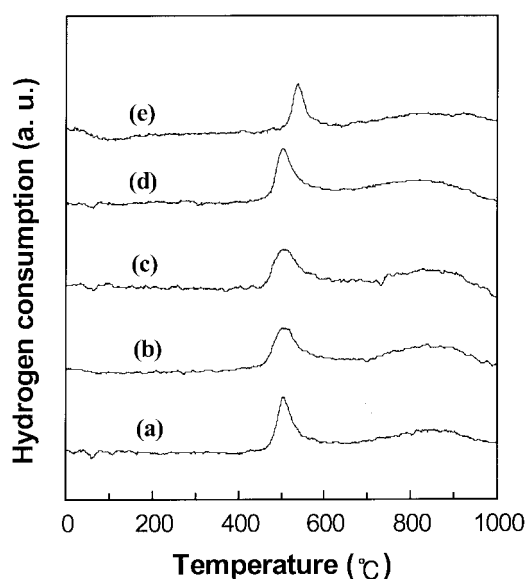
**Table 1.** CO Conversion of Various Catalysts

Catalyst	Reaction temp. (°C)	CO conversion (%)
Fe-Cr (commercial)	450 °C	30
Cu-Zn (commercial)	200 °C	57
10K3C10M	450 °C	54

catalyst (commercial) and Cu-Zn catalyst (commercial). Reaction temperature and CO conversion are shown in Table 1. In our experiments, 10K3C10M catalyst showed similar catalytic activity to that of Cu-Zn catalyst that has been known as the most active catalyst for water gas shift reaction.

**Characterization of Catalysts:** TPR experiments were performed to examine the effect of the addition of K on the reducibility of the catalysts. In the previous study, we found that the reducibility of a catalyst was closely related to the activity for water gas shift reaction in Mo, CoMo, and NiMo systems and catalysts with better reducibility showed better activities. Figure 3 shows TPR profiles of xK3C10M catalyst similar to those of Mo and CoMo catalysts. There were lower temperature peak between 500-600 °C and higher temperature peak between 800-950 °C. We identified the lower and higher temperature peaks as the reduction of MoO<sub>3</sub> to MoO<sub>2</sub> and MoO<sub>2</sub> to Mo, respectively. We observed that the addition of Co shifted the lower temperature peak from 566 °C to 538 °C. This suggested that the enhanced activity of CoMo for water gas shift reaction was attributed to the better reducibility resulting from the addition of Co. The addition of K did not enhance the reducibility of 3C10M catalyst but shifted lower temperature peak to higher temperature when a large amount of K was added. From this result, we concluded that the addition of K did not enhance the reducibility of 3C10M catalyst and there were another factors related to the catalytic activity.

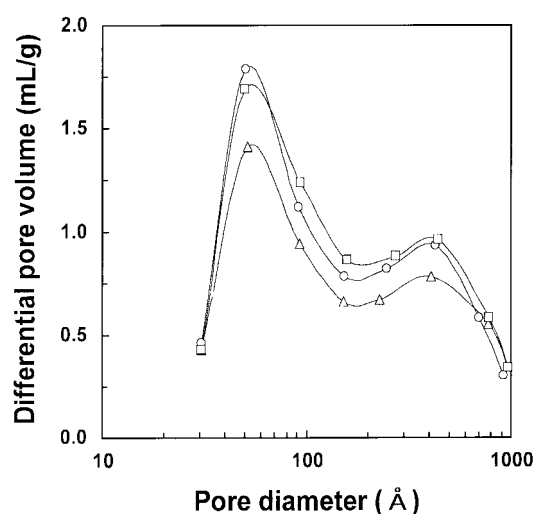
BET specific surface areas of samples are shown in Table

**Figure 3.** TPR profiles of (a) 3C10M, (b) 5K3C10M, (c) 10K3C10M, (d) 25K3C10M, and (e) 50K3C10M.**Table 2.** BET Surface Area of xK3C10M Catalysts

Catalyst	BET S. A. (m <sup>2</sup> /g)
$\gamma$ -Al <sub>2</sub> O <sub>3</sub>	193
3C10M	164
5K3C10M	178
10K3C10M	189
25K3C10M	184
50K3C10M	180

2. The surface area of 3C10M decreased compared with that of a support itself due to the pore blocking and surface smoothing by the deposition of metal oxide on the support. Giordano *et al.* also reported the surface area of catalysts decreased with the increase of an MoO<sub>3</sub> loading amount.<sup>17</sup> We observed that the addition of K increased the surface area of the catalysts compared with that of 3C10M. This implied that the addition of K was beneficial to the dispersion of large metal oxide agglomerates to small metal oxide particles on the support. Figure 4 shows the pore size distributions of  $\gamma$ -Al<sub>2</sub>O<sub>3</sub>, 3C10M, and 5K3C10M. This also showed that the addition of K regenerated the blocked pores, which gave K added catalyst almost the same pore structure as that of the support,  $\gamma$ -Al<sub>2</sub>O<sub>3</sub>. We observed that the addition of K was not beneficial when Co and Mo did not coexist. In summary, the role of K was to help the association between Mo oxide and Co oxide on the support so that the catalyst had more active sites resulting from chemically combined Co-Mo as well as enhanced surface area. XRD analysis was performed for the characterization of metal oxides on the catalysts, however, no characteristic XRD peaks of metal oxides were detected due to a low loading amount of the metal oxides. Meanwhile, weak MoO<sub>3</sub> peaks were observed when 30 wt% of MoO<sub>3</sub> was loaded.

Raman laser spectroscopy was applied. Because supports such as alumina and silica shows no specific peak in Raman analysis, Raman analysis is a useful tool for the analysis of a supported catalyst with a low amount of metal loading. Fig-

**Figure 4.** Pore size distributions of catalysts (○:  $\gamma$ -Al<sub>2</sub>O<sub>3</sub>, △: 3C10M, □: 5K3C10M).

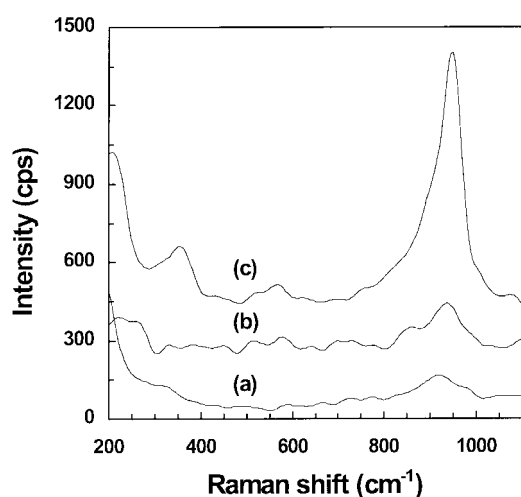


Figure 5. Raman spectra of (a) 5M, (b) 10M, and (c) 30M.

Figure 5 shows Raman spectra of 5M, 10M, and 30M. The peak at  $920\text{ cm}^{-1}$  shifted to  $950\text{ cm}^{-1}$  with the increase of an  $\text{MoO}_3$  loading amount. Kim *et al.* reported that the peak at  $938\text{--}941\text{ cm}^{-1}$  resulted from the symmetric stretching of octahedrally coordinated terminal  $\text{Mo}=\text{O}$  in  $\text{Mo}_7\text{O}_{24}^{6-}$ , and peak at  $320\text{ cm}^{-1}$  resulted from the bending of tetrahedrally coordinated isolated  $\text{Mo}-\text{O}$  in  $\text{MoO}_4^{2-}$ .<sup>18</sup> It could be suggested that the amount of  $\text{Mo}_7\text{O}_{24}^{6-}$  increased with the increase of an Mo loading amount, which was also confirmed by TPR and BET surface area analyses. Stencel *et al.* reported that the peaks did not shift to higher wave number when catalysts were not in contact with air after calcination.<sup>19</sup> He concluded that the moisture in air reacted with a metal oxide to affect the stretching frequency of terminal  $\text{Mo}=\text{O}$ . This peak shift was commonly observed in  $\text{MoO}_3$ ,  $\text{WO}_3$ , and  $\text{V}_2\text{O}_5$  supported on  $\text{TiO}_2$  and  $\text{Al}_2\text{O}_3$ . Figure 6 shows Raman spectra of 10M, 3C10M, and 5K3C10M. The peak at  $940\text{ cm}^{-1}$  was observed in 10M, and the peak still remained when 3C was added to 10M, however, drastic decrease of the peak area was observed when K was added. This could be an evidence that the large  $\text{Mo}_7\text{O}_{24}^{6-}$  cluster was divided into smaller metal oxide cluster. In addition, the peak at about  $300\text{ cm}^{-1}$  resulting from  $\text{MoO}_4^{2-}$  increased when K was added.

TEM and EDP analyses were performed to get the information of a particle size and crystal structure of metal oxides on the catalysts. Figure 7 shows TEM images of the catalysts. No noticeable difference among the catalysts was observed with TEM images ( $\times 50,000$ ). EDP result showed a difference between 3C10M and 5K3C10M. For alumina, there was no diffraction pattern except bright rings, while for 3C10M, there was a clear diffraction pattern attributed to well developed crystal structure, and for 5K3C10M, there was also a diffraction pattern which was fainter than that of 3C10M. In general, a brighter and clearer diffraction pattern denotes well developed large crystal structure. From these results, we suggested that there were developed metal oxide crystals on 3C10M even though it was not detected by XRD and the addition of K decreased the crystallinity of the metal

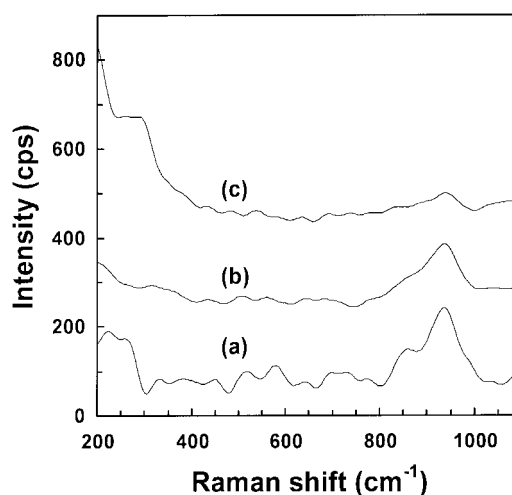


Figure 6. Raman spectra of (a) 10M, (b) 3C10M, and (c) 5K3C10M.

oxides by decreasing the size of the oxides.

**Kinetic Study:** Figure 8 shows Arrhenius plots of 3C10M and 5K3C10M for water gas shift reaction at 300, 350, 400, and 450 °C. A following equation was used to determine the reaction constant  $k$  and the reaction order was assumed to be first order with respect to CO because the amount of water was in excess.

$$-\ln \left[ \frac{X_{\text{CO}} - X_{\text{CO}}^{\text{eq}}}{X_{\text{CO}}^{\text{o}} - X_{\text{CO}}^{\text{eq}}} \right] = k \frac{V}{F}$$

( $V$  = volume of a catalyst,  $F$  = flow rate of reactant gases,  $X_{\text{CO}}^{\text{o}}$  = initial CO mole fraction,  $X_{\text{CO}}$  = final CO mole fraction,  $X_{\text{CO}}^{\text{eq}}$  = mole fraction of CO at equilibrium, and  $k$  = first order rate constant)

Activation energies of 3C10M and 5K3C10M were 43.1 and 47.8 kJ/mole and frequency factors were 4,297 and 13,505  $\text{sec}^{-1}$ , respectively. The addition of K gave larger activation energy and larger frequency factor, which was well matched with the TPR result that the addition of K retarded reducibility of CoMo catalysts and also matched with larger BET surface area of CoMo catalysts when K was added. This implied that the enhanced activity of 5K3C10M for water gas shift reaction was attributed to the increase of the number of active sites rather than the change of activation energy. These results were well correlated with other results obtained from Raman spectroscopy and EDP analyses.

**Effect of a Support:** We suggested that the addition of K enhanced the dispersion of metal oxide and retarded the reducibility. There are two possible explanations for the role of K. One is direct interaction of K with surface metal oxides and the other is the interaction of K with the support,  $\gamma\text{-Al}_2\text{O}_3$  leading to the change of properties of surface metal oxides. Bulk xK3C10M catalysts were prepared to study the effect of the support on the role of K in cobalt-molybdenum catalyst. These catalysts were prepared by calcination of mixed metal salts which were the same as the salts used for

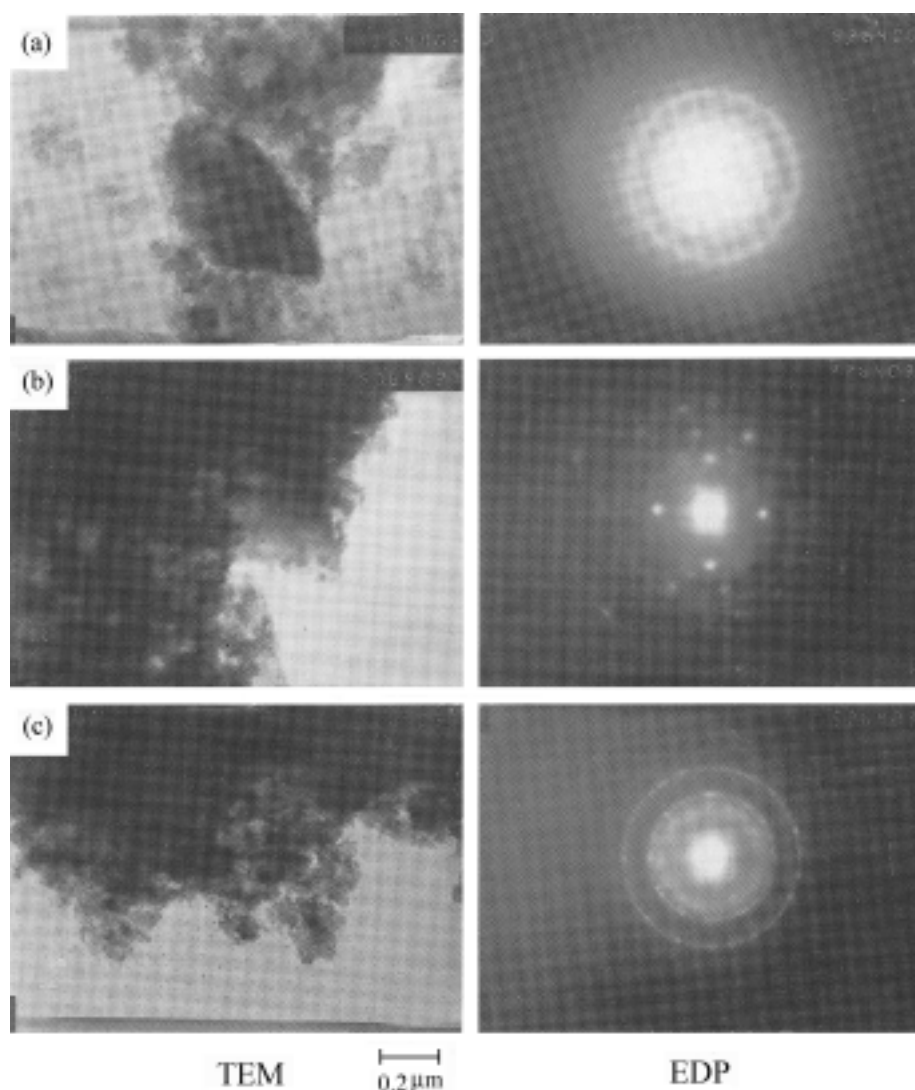


**Figure 7.** TEM images and electron diffraction patterns of (a)  $\gamma$ -Al<sub>2</sub>O<sub>3</sub>, (b) 3C10M, and (c) 5K3C10M.

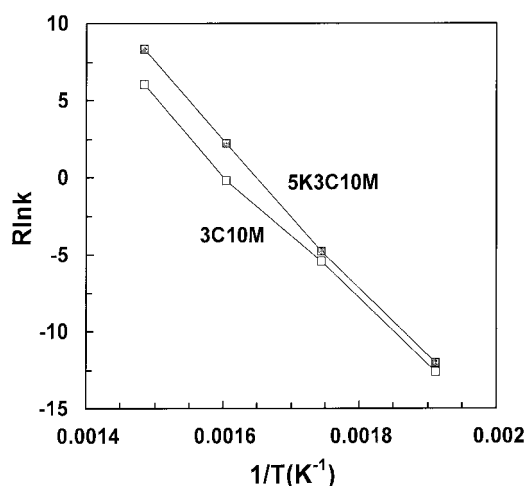


**Figure 8.** Arrhenius plots of 3C10M and 5K3C10M.

the impregnation of each component. Figure 9 shows TPR profiles of bulk xK3C10M catalysts. The addition of K gave

complicated TPR patterns, especially in lower temperature range. There was a separation of lower temperature peak into several peaks by the increase of the amount of K, which meant there were more than two kinds of oxygen species with different environment to be reduced at low temperature. In the case of bulk samples, the addition of K seemed to enhance the reducibility of the catalysts, which was the opposite of the result with supported catalysts. This could be explained that the enhanced dispersion gave stronger interaction between the support and surface metal oxides and it retarded the reducibility of the supported metal oxides. Figure 10 shows XRD patterns of these bulk catalysts. MoO<sub>3</sub> and CoMoO<sub>4</sub> were observed in 3C10M. The relative amount of MoO<sub>3</sub> to CoMoO<sub>4</sub> was increased by the addition of K. In the case of the addition of excess K, 50K3C10M, K<sub>0.3</sub>MoO<sub>3</sub> was formed and MoO<sub>3</sub> almost disappeared. The formation of K<sub>0.3</sub>MoO<sub>3</sub> was plausible considering the ratio of K to Mo. Kettmann *et al.* reported the formation of K<sub>2</sub>Mo<sub>2</sub>O<sub>7</sub>, however, they used a large amount of K (K: 8.4 g, Co: 1.4 g, and Mo: 4.4 g for the 100 g of catalyst).<sup>14</sup> From these observa-

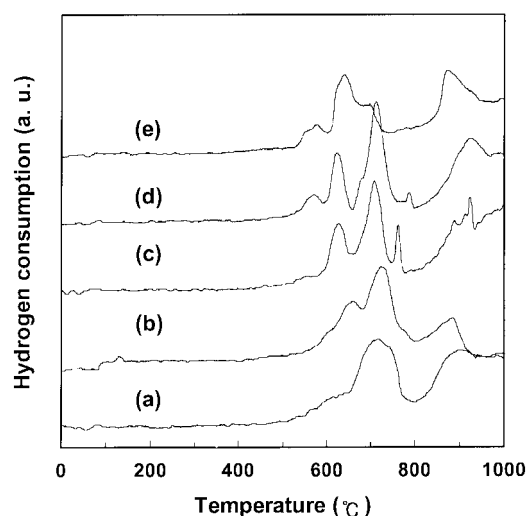


Figure 9. TPR profiles of bulk catalysts (a) 3C10M, (b) 1K3C10M, (c) 5K3C10M, (d) 10K3C10M, and (e) 50K3C10M.

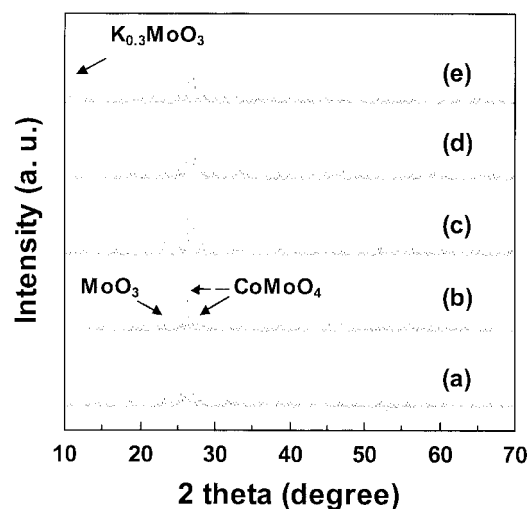


Figure 10. XRD patterns of bulk catalysts (a) 3C10M, (b) 1K3C10M, (c) 5K3C10M, (d) 10K3C10M, and (e) 50K3C10M.

tions, we suggested that the effect of K was the result of the interaction between K and CoMo oxides irrelevant to the support.

### Conclusions

The catalyst with 10 at% of K to Mo atoms in 3C10M, the catalyst added 3 wt% CoO to 10 wt% MoO<sub>3</sub>/γ-Al<sub>2</sub>O<sub>3</sub>, showed the highest activity for water gas shift reaction. The addition of K retarded the reducibility of cobalt-molybdenum catalysts. It gave, however, good dispersion and large BET surface area to the catalysts which were attributed to the disappearance of polymolybdate cluster such as Mo<sub>7</sub>O<sub>24</sub><sup>6-</sup>

and the formation of small MoO<sub>4</sub><sup>2-</sup> cluster. It was confirmed by the analyses of pore size distribution, activation energy, Raman spectroscopy, and electron diffraction. The activation energies and the frequency factors of the catalysts 3C10M and 5K3C10M (the catalyst added 5 at% K for Mo to the catalyst 3C10M) were 43.1 and 47.8 kJ/mole, and 4,297 and 13,505 sec<sup>-1</sup>, respectively. These values were also well correlated with our suggestion. These phenomena were attributed to the direct interaction between K and CoMo oxides irrelevant to the support.

**Acknowledgment.** This paper was supported by NON DIRECTED RESEARCH FUND, Korea Research Foundation. The authors would like to thank both KRF for financial support and Catalysis Society of Japan for supplying γ-alumina as a support.

### References

1. Probst, R. F.; Hicks, R. E. *Synthetic Fuels*; McGraw-Hill: London, U. K., 1982; p 144.
2. Twigg, M. W. *Catalyst Handbook*; Wolfe Publishing Ltd.: London, U. K., 1989; p 283.
3. Newsome, D. S. *Catal. Rev.-Sci. Eng.* **1980**, *21*, 275.
4. Bohlbro, H.; Jorgensen, M. H. *Chem. Eng. World* **1970**, *5*, 46.
5. Tsuchimoto, T.; Morita, Y.; Yamamoto, K. *Kogyo Kagaku Zasshi* **1968**, *71*, 1484.
6. Li, Y.; Wang, R.; Chang, L. *Catal. Today* **1999**, *51*, 25.
7. Andreev, A. A.; Kafedjiyski, V. J.; Edreva-Kardjieva, R. *M. Appl. Catal. A* **1999**, *179*, 223.
8. Kim, J. -H.; Lee, H. -I. *J. Korean Chem. Soc.* **1998**, *42*, 696.
9. Park, J. -N.; Kim, J. -H.; Lee, H. -I. *Bull. Korean Chem. Soc.* submitted.
10. Ramaswamy, A. V.; Sivasanker, S.; Ratnasamy, P. *J. Catal.* **1976**, *42*, 107.
11. Lycourghiotis, A.; Vattis, D.; Karaiskakis, G.; Katsanos, N. *J. Less-Common Met.* **1982**, *86*, 137.
12. Kordulis, C.; Voliotis, S.; Lycourghiotis, A. *J. Less-Common Met.* **1982**, *84*, 187.
13. Kantschewa, M.; Delannay, F.; Jeziorowski, H.; Delgado, E.; Eder, S.; Ertl, G.; Knözinger, H. *J. Catal.* **1984**, *87*, 482.
14. Kettmann, V.; Balgavy, P.; Sokol, L. *J. Catal.* **1988**, *112*, 93.
15. Xie, X.; Yin, H.; Dou, B.; Huo, J. *Appl. Catal.* **1991**, *77*, 187.
16. Park, J. -N.; Kim, J. -H.; Lee, H. -I. *Bull. Korean Chem. Soc.* **1998**, *19*, 1363.
17. Giordano, N.; Bart, J. C. J.; Vaghi, A.; Castellan, A.; Martinotti, G. *J. Catal.* **1975**, *36*, 81.
18. Kim, D. S.; Segawa, T.; Soeya, T.; Wachs, I. E. *J. Catal.* **1992**, *136*, 539.
19. Stencel, J. M.; Makovsky, L. E.; Sarkus, T. A.; de Vries, J.; Thomas, R.; Moulijn, J. A. *J. Catal.* **1984**, *90*, 314.